

Multi-Functional Probe Recording: Field-Induced Recording and Near-Field Optical Readout

Kang-Ho Park, Jeongyong Kim, Ki-Bong Song, Sung-Q Lee, Junho Kim, and Eun-Kyoung Kim

We demonstrate a high-speed recording based on field-induced manipulation in combination with an optical reading of recorded bits on Au cluster films using the atomic force microscope (AFM) and the near-field scanning optical microscope (NSOM). We reproduced 50 nm-sized mounds by applying short electrical pulses to conducting tips in a non-contact mode as a writing process. The recorded marks were then optically read using bent fiber probes in a transmission mode. A strong enhancement of light transmission is attributed to the local surface plasmon excitation on the protruded dots.

Keywords: atomic force microscope (AFM), near-field scanning optical microscope (NSOM), probe, high speed recording, near-field optical readout.

I. Introduction

The application of the atomic force microscope (AFM) for data storage has been extensively explored for a high density recording of \sim Tb/in². A number of AFM writing and reading methods showing the μ s recording time and nano-scale bit size were reported. However, contact problems such as tip instability, bit erasure caused by damage to the tip, or degradation of the media, still remain in realizing reliable and practical data storage using local probe technology [1]-[3]. Near-field scanning optical microscopy (NSOM) appears to be an alternative technology because sub-100-nm bits can be optically recorded and read in a non-contact mode [4], [5]. However, due to the low-light throughput of an NSOM probe and the resultant low-data recording rate, it is still far from being practically used. Therefore, it seems pertinent to combine the high-speed writing capability of AFM with the advantages of non-degradable NSOM readout for the realization of reliable high density SPM data storage. We propose a hybrid nano-recording mechanism, which we call a multi-functional probe recording (MPR) technique, that combines AFM recording and an NSOM optical reading. In an ideal MPR system, recording and reading should be done with a single multifunctional probe, but in our preliminary experiment, recording and reading is performed with AFM and NSOM, respectively.

By using the MPR technique, we have an advantage in selecting the recording media because recording is not limited in the photonic mode. We made tens of nm-sized recording marks on gold films by applying short electric pulses to a conducting AFM probe. In order to minimize damage to both the tip and sample during the recording, we introduce a non-contact AFM configuration. This allows us to locally heat the

Manuscript received May 15, 2003; revised Jan. 16, 2004.

This work was supported by MOST under the R&D program for fusion strategy of advanced technology, Korea.

Kang-Ho Park (phone: +82 42 860 6028, email: pkh@etri.re.kr), Ki-Bong Song (email: kbsong@etri.re.kr), Sung-Q Lee (email: Hermann@etri.re.kr), Junho Kim (email: jhk@etri.re.kr), and Eun-Kyoung Kim (email: eunkk@etri.re.kr) are with Basic Research Laboratory, ETRI, Daejeon, Korea.

Jeongyong Kim (email: jeongyong@incheon.ac.kr) is with Department of Physics, University of Incheon, Incheon, Korea.

Au surface using the field-emission current [6] from the sharp and hard W_2C coated tip and to manipulate the Au atoms or clusters without a mass transfer between the tip and sample [7], [8]. The recorded marks are then optically read out by using NSOM probes with a 100-nm spatial resolution.

II. Experiments

In the case of a Si substrate, we prepared a clean p-type Si (100) sample with a resistivity of $1 \Omega\text{-cm}$ using repeated flashing at 1150°C in a UHV ($\sim 1 \times 10^{-10}$ Torr) chamber. We then transferred it to the deposition chamber. We evaporated Au onto the Si sample in the presence of an Ar background gas at a pressure of 0.3 to 3 mbar. As a result of collisions between the effusing Au atoms, or between small clusters and Ar atoms, a supersaturation of the metal vapor was produced leading to the nucleation and condensation of the uniform Au clusters. The average particle size is sensitive to evaporation conditions such as the pressure of the Ar background gas, evaporation rate, and the distance between the evaporator and the sample substrate [9]. The Au films could be deposited on a glass substrate by a plain evaporation method at a high vacuum of $\sim 1 \times 10^{-7}$ Torr for the comparative study. As an adhesion layer, we deposited Ti of 1 to 2 nm prior to the deposition of the Au to enhance the adhesion between the SiO_2 film and the Au layer and to reduce the roughness of the Au surface. The Ti and Au were successively deposited using e-beam evaporation under an operation pressure of less than 10^{-6} Torr on glass. The sample was then transferred to the AFM stage in air.

Figure 1 shows the experimental layout. The experimental procedure consists of two steps, (a) AFM field-induced recording and (b) an optical reading by an NSOM probe. We modified a commercial AFM (PSIA CP-research) to carry out both operations. Because the application bias voltage was limited to up to ± 10 V in our AFM system, we used an extra voltage amplifier to amplify the bias voltage to ± 100 V in order to achieve the field. Commercially available W_2C coated tips were used due to their hardness and high melting point. We recorded the sample current, amplified using an extra current amp, in a PC via the auxiliary channel of an AFM control unit. The gap control between the probe and the sample surface was carried in general AFM noncontact mode using the vibrating cantilever under feedback control. The vibration frequency is typically set at 170 to 200 KHz. For the NSOM reading, a bent optical fiber probe (Nanonics) was installed in place of an AFM probe. We fabricated $100 \times 100 \times 15 \mu\text{m}$ mirrors and attached them on cantilever probes to improve the quality of the reflected laser beam. By doing this, the shape of the laser beam reflected from the micro-mirror on the cantilever probe edge became circular, providing enough intensity and sensitivity. As a result, we

obtained sharp resonance peaks at 80 to 100 kHz with a Q factor of 50 to 100, showing that our bent NSOM probe is capable of non-contact mode imaging, just like ordinary AFM probes. We launched laser light, modulated at a few kHz for lock-in amplification, into the other end of the fiber and illuminated the evanescent light from the aperture of probe onto the sample. For the detection of transmitted light through the sample, we placed a small planar silicon photodiode (4×4 mm) under the sample. Our light detection system is quite simple, without the need of collection optics or a highly sensitive avalanche photodiode. The topography and the optical illumination image were simultaneously obtained. We used a 635-nm laser diode or 514-nm Ar ion laser for the NSOM reading.

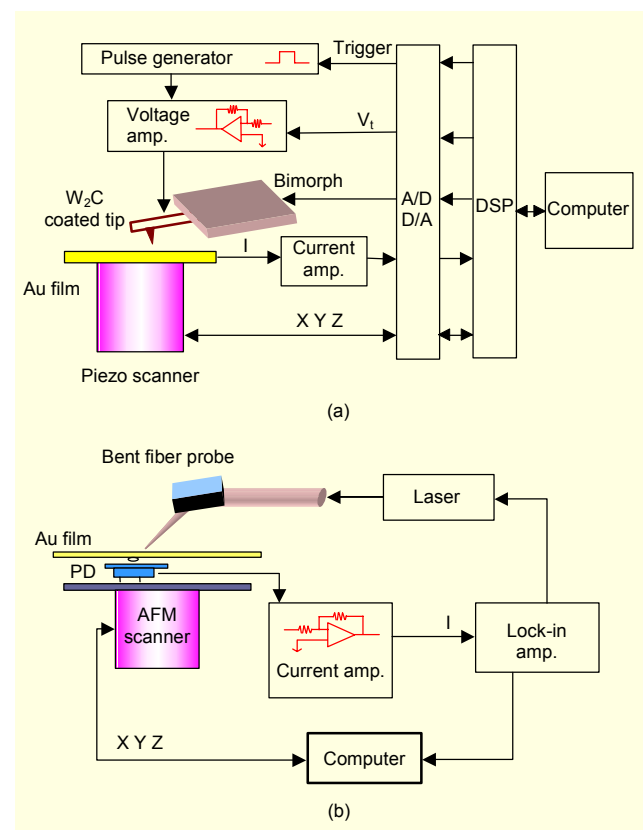


Fig. 1. Schematic diagram of a multifunctional probe recording apparatus. (a) An AFM field-induced recording and (b) an NSOM reading setup.

III. Results and Discussion

1. AFM Writing

Figure 2(a) shows an AFM image of a granular 30-nm thick Au film. Upon depositing the Au at a background gas pressure of 0.3 mbar, a heater-sample distance of 5 cm, and a deposition rate of 0.3 nm/min, we uniformly distributed Au nanoclusters

on the surface. The size distributions of the Au clusters are 25 nm in diameter and 10 nm in height at a nominal coverage of 30 nm estimated using a crystal thickness monitor. By applying a tip voltage pulse of -40V with a pulse duration of 100 msec under feedback control, the mounds, up to 90 nm in width and up to 15 nm in height, were created reproducibly, as displayed in Fig. 2(b). The lines of 60 nm in width can even be reproducibly fabricated using a similar procedure. Figure 3 shows the example of the fabricated line structure. We fabricated both the line structure and the 60-nm lines using a tip voltage of -50V and a continuous constant current of 50 pA, while moving the tip with a constant speed of 160 nm/s under feedback control along the line. The granular nature of the cluster network was preserved in dots and lines after the fabrication, showing that a non-contact fabrication mechanism was involved. For instance, the three clusters, *a*, *b*, and *c* shown in Fig. 2(a), are found to be lifted and agglomerated into the mound in the upper-left corner of Fig. 2(b), which is strong evidence of a field gradient-induced diffusion mechanism [10] without the event of contact between the tip and the sample.

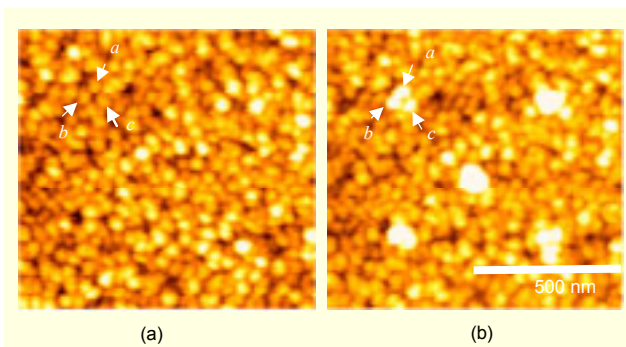


Fig. 2. (a) An AFM image of Au granular films of 30 nm thickness grown on a Si substrate by a gas evaporation method. (b) An AFM image after the fabrication of five mounds. The cluster *a*, *b*, *c* are lifted and agglomerate on the mound in the upper-left corner ($V_{\text{tip}} = -40\text{V}$, $T_{\text{pulse}} = 100\text{ms}$).

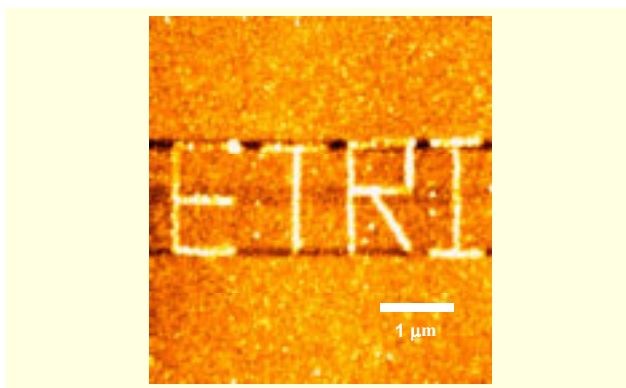


Fig. 3. A field-emission-induced fabrication of the word “ETRI” ($V_{\text{tip}} = -50\text{V}$, $I = 50\text{pA}$, $V_{\text{scan}} = 160\text{nm/s}$).

Those fabrication events occur only when the current flows. The fabrication depends on the condition of the tip edge, such as its conductivity or shape, because the field emission current is very sensitive to the condition of the tip edge. In the case of highly conductive tips, the mounds could be formed very quickly with low bias voltages such as 20 to 30 V. But in this case, the fabrication of the line was impossible. This can be explained as fabrication interruption by the abrupt retract of the tips due to the contact between the protruding mounds and the tip itself in the presence of the feedback operation during the line fabrication. Accordingly, slow fabrication compared with the feedback response time (10 to 100 μsec) seems to be a criteria for a perfectly non-contact manipulation mechanism between the tip and the sample. The fabrication behavior is also sensitive to the kind of substrate matter. In the case of glass substrates, the fabrication is routinely possible in conditions of low bias and a short pulse duration. The tip voltage pulse of -20 to -30V with a pulse duration of 20 to 100 μsec was found to be suitable for fabrication without serious damage to the tip's edge. The conductivity difference is not a plausible origin of the fast writing in a glass substrate because the film resistance is nearly same in both films (up to 5 Ω).

Field emission-induced local heating and concurrent field gradient-induced diffusion are the most probable mechanisms for the formation of nanoscale mounds. Figure 4 shows the schematics for the non-contact, field-induced fabrication mechanism of a mound structure. The local temperature in the area covered by the flow of field-emitted electrons from the sharp tip increases, as shown in Fig. 4(a), and the Au clusters or atoms can move toward the tip on the surface [7]. Finally, the mound structure composed of the migrated clusters or atoms is formed, as shown in Fig. 4(b). The point contact or field evaporation is not a plausible mechanism for a mound formation because the formation of the craters or pits are not observed as such in typical Au surfaces with hard tungsten tips [11]. Also, the current is not as large as in point contact during the fabrication. Likewise, in the case of reverse polarity, we found the fabrication of the mounds does not reliably occur, and the critical bias voltage is larger than in the case of a negative tip bias. The substrate dependence of the fabrication can be explained by the difference of heat dissipation in each material. Because the thermal conductivity k of glass ($0.014\text{Wcm}^{-1}\text{K}^{-1}$) is much lower than that of Si ($1.48\text{Wcm}^{-1}\text{K}^{-1}$) [12], the local temperature in the e-beam area could be highly enhanced. We roughly estimated the local temperature increase ΔT to be 22.7 K in the case of a glass substrate [13]. It is calculated by the equation of $\Delta T \cong VI/4\pi kl$, where $V = 24\text{V}$, moderate current condition such as $I = 1\text{nA}$, $k = 0.014\text{Wcm}^{-1}\text{K}^{-1}$ at 300 K, mean free path $l = 6 \times 10^{-8}\text{cm}$ in glass. It is quite large in contrast to the negligible temperature increase in the tunneling regime on metal surfaces. The fast fabrication with

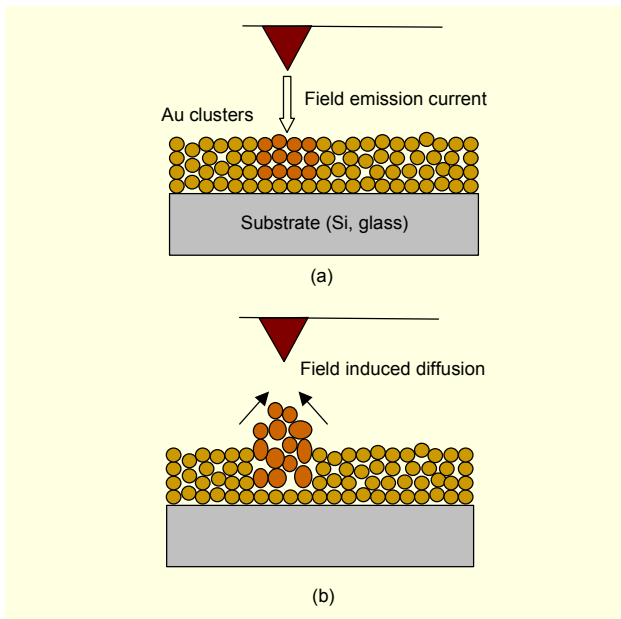


Fig. 4. A schematic diagram of (a) a field-emission-induced local heating and (b) a field induced migration of Au clusters by the voltage application between the conducting AFM probe and the granular sample.

the lower bias voltages in the glass substrate can be explained as the distinct increase in local temperature, which is induced by the suppression of the heat dissipation.

2. NSOM Reading

Such fabricated mound structures on glass can be used as the information recording marks for an NSOM reading because they are morphologically protruded on a nanometer scale, and the optical transmission on the nanoscale mounds are significantly enhanced due to the surface plasmon coupling on the protruding structures [14]. After formation of the recording marks, we mounted the sample on an NSOM setup and changed the tip from a standard AFM probe to a bent optical fiber probe. Figure 5 displays three images of typical recording dots on a glass substrate: (a) a topography using an AFM probe, (b) a topography using an NSOM probe, and (c) an optical transmission generated using a bent optical fiber probe. It should be noted that the array of recorded dots appear as bright spots in an optical transmission image with a spatial resolution of about 100 nm [15]. We estimate the optical signal increase at the mark to be 30% of the background signal. To make sure the observed optical contrast is not made up of the artifacts caused by cross-talk due to tip movement, we performed a “constant height mode (CHM)” NSOM, where the probe keeps the same height rather than following the surface corrugation, such as in “constant gap mode (CGM)” [16], [17]. The bright spot was

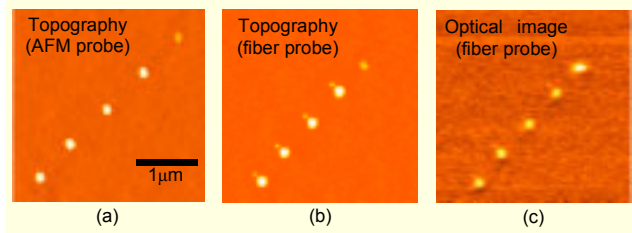


Fig. 5. A dot array fabricated by a field-induced method on a Au thin film grown on a glass substrate ($V_{tip} = -24$ V, $T_{pulse} = 20$ μ s): (a) an AFM image, (b) a topography using an NSOM probe, and (c) an NSOM optical transmission image.

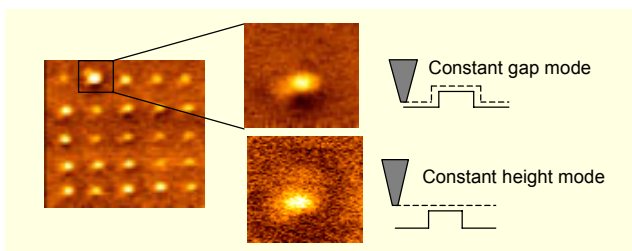


Fig. 6. An NSOM optical transmission image on a selected dot by using both a constant gap mode and constant height mode, respectively.

still observed in the CHM with the same intensity as in CGM, confirming that the observed bright spots make up a real optical contrast, as shown in Fig. 6.

Of interest is the enhancement of light transmission at the recording marks. One possible explanation is the excitation of surface plasmon on the recording marks, where the evanescent field emanated from the probe is coupled to the surface plasmon on the recording marks and re-emitted as a propagating wave to the far field [18], which also results in a throughput enhancement of the NSOM probes [19]. Such a role for the surface plasmon in NSOM imaging, as found in the field enhancement around metal mounds, has been extensively investigated [18]. To confirm the existence of surface plasmon, it would be necessary to obtain a full absorption spectra over a broad wavelength range and look for the scattering resonance [20].

As a preliminary investigation, we used two lasers of different wavelengths, 635 and 514 nm, for NSOM readings of a selected array of recording dots, and compared the resultant NSOM optical images. The result is displayed in Fig. 7. The images in Figs. 7(b) and (c) are obtained using a 635-nm laser diode and a 514-nm Argon ion laser. Both images look almost the same except that in Fig. 7(b), the brightest spot is the uppermost small recording dot *a* while in Fig. 7(c) the lowermost large recording dot *b* looks the brightest. We found that there is no serious heterogeneity in the NSOM images except for a slight time-dependent variation of the PD signal.

The upper area has a brighter background compared to the lower area in Figs. 7(b) and (c) due to the time dependent variation. But the contrast change manifests from the dramatic difference between the brightness of dots *a* and *b* under the similar aspect of the brightness gradient of the background. The evidence of an absence of serious heterogeneity can be found in our previous papers showing NSOM images using the same detector [14], [15]. The varying optical images with an incident laser wavelength reveals that the optical contrast of the NSOM images is dependent on the wavelength of the incident light, implying a resonance behavior. Further investigation will be needed to fully understand the plasmon excitation mechanism on the recording marks.

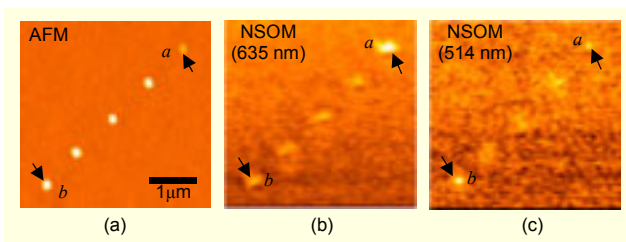


Fig. 7. AFM and NSOM images of an array of recorded marks: (a) an AFM topography, (b) an NSOM image using a laser diode at 635 nm, and (c) an NSOM image using an Ar ion laser at 514 nm. It should be noted that the change of laser wavelength leads to the different optical contrast at each recorded dot, *a* and *b*, which is probably due to the variation of the dot shapes.

IV. Conclusion

We have devised a new reliable recording mechanism based on field induced electron emission and a concurrent migration of atoms and clusters on metal films without a contact process between the tip and sample materials. This non-contact mechanism has advantages such as the minimization of damage or consumption of tip matter over the previously devised field evaporation and contact mechanism. They can be applied to an MPR technique that combines high-speed AFM recording with an optical reading using NSOM. As a preliminary result, we produced sub-100-nm recording marks on gold granular films by applying an electrical voltage to W_2C coated probes in AFM NC mode, and used NSOM for an optical reading with a 100-nm spatial resolution. We observed an enhancement of the optical transmission on the recording marks possibly due to the local surface plasmon excitation. For completion of the MPR technique, the recording and reading processes demonstrated here need to be integrated into a single process by developing MPR probes capable of both AFM recording and NSOM reading.

References

- [1] G. Binnig, M. Despont, U. Drechsler, W. Häberle, M. Lutwyche, P. Vettiger, H.J. Mamin, B.W. Chui, and T.W. Kenny, "Ultrahigh-Density Atomic Force Microscopy Data Storage with Erase Capability," *Appl. Phys. Lett.*, vol. 74, 1999, pp. 1329-1331.
- [2] M.I. Lutwyche, M. Despont, U. Drechsler, U. Dürig, W. Häberle, H. Rothuizen, R. Stutz, R. Widmer, G. Binnig, and P. Vettiger, "Highly Parallel Data Storage System Based on Scanning Probe Arrays," *Appl. Phys. Lett.*, vol. 77, 2000, pp. 3299-3301.
- [3] K. Yano and T. Ikeda, "Stable Bit Formation in Polyimide Langmuir-Blodgett Film Using Atomic Force Microscope," *Appl. Phys. Lett.*, vol. 80, 2002, pp. 1067-1069.
- [4] E. Betzig, J.K. Trautman, R. Wolfe, E.M. Gyorgy, P.L. Finn, M.H. Kryder, and C.H. Chang, "Near-Field Magneto-Optics and High Density Data Storage," *Appl. Phys. Lett.*, vol. 61, 1992, pp. 142-144.
- [5] S. Hosaka, T. Shintani, M. Miyamoto, A. Hirotsune, M. Terao, M. Yoshida, K. Fujita, and S. Kämmer, "Nanometer-Sized Phase-Change Recording Using a Scanning Near-Field Optical Microscope with a Laser Diode," *Jpn. J. Appl. Phys.*, vol. 35, 1996, pp. 443-447.
- [6] K. Wilder, C.F. Quate, D. Adderton, R. Bernstein, and V. Elings, "Noncontact Nanolithograph Using the Atomic Force Microscope," *Appl. Phys. Lett.*, vol. 73, 1998, pp. 2527-2529.
- [7] K.-H. Park, J.S. Ha, W.S. Yun, and Y.-J. Ko, "Selective Manipulation of Ag Nanoclusters on a Passivated Silicon Surface," *Jpn. J. Appl. Phys.*, vol. 39, Part 1, 2000, pp. 4629-4630.
- [8] K.-H. Park, M. Shin, J.S. Ha, W.S. Yun, and Y.-J. Ko, "Fabrication of Lateral Single Electron Tunneling Structures by Field-Induced Manipulation of Ag Nanoclusters on a Silicon Surface," *Appl. Phys. Lett.*, vol. 75, 1999, pp. 139-141.
- [9] A. Werner and H. Hibst, "Particulate Au and Ag Films for Optical Recording," *Appl. Opt.*, vol. 28, 1989, pp. 1422-1428.
- [10] T.T. Tsong, "Effects of an Electric Field in Atomic Manipulations," *Phys. Rev. B*, vol. 44, 1991, pp. 13703-13710.
- [11] T.C. Chang, C.S. Chang, H.N. Lin, and T.T. Tsong, "Creation of Nanostructures on Gold Surfaces in Nonconducting Liquid," *Appl. Phys. Lett.*, vol. 67, 1995, pp. 903-905.
- [12] C. Kittel, *Introduction to Solid State Physics*, Wiley & Sons, 1986, pp. 110 and 508.
- [13] B. N. J. Persson and J. E. Demuth, "Inelastic Electron Tunneling from a Metal Tip," *Solid State Comm.*, vol. 57, 1986, pp. 769-772.
- [14] J. Kim, K.-B. Song, and K.-H. Park, "Near-Field Optical Readout Combined with Atomic Force Probe Recording," *Jpn. J. Appl. Phys.*, vol. 41, Part 1, 2002, pp. 1903-1904.
- [15] J. Kim, K.-B. Song, K.-H. Park, H.W. Lee, and E. Kim, "Simple Near-Field Optical Recording Using Bent Cantilever Probes," *ETRI J.*, vol. 24, 2002, pp. 205-210.
- [16] B. Hecht, H. Bielefeldt, Y. Inouye, and D.W. Pohl, "Facts and Artifacts in Near-Field Optical Microscopy," *J. Appl. Phys.*, vol. 81, 1997, pp. 2492-2498.
- [17] C.E. Jordan, S.J. Stranick, L.J. Richter, and R.R. Cavanagh,

“Removing Optical Artifacts in Near-Field Scanning Optical Microscopy by Using a Three-Dimensional Scanning Mode,” *J. Appl. Phys.*, vol.86, 1999, pp. 2785-2789.

- [18] T. Klar, M. Perner, S. Grosse, G. von Plessen, W. Spirkl, and J. Feldmann, “Surface Plasmon Resonances in Single Metallic Nanoparticles,” *Phys. Rev. Lett.*, vol. 80, 1998, pp. 4249-4252.
- [19] T. Yatsui, M. Kourogi, and M. Ohtsu, “Highly Efficient Excitation of Optical Near-Field on an Apertured Fiber Probe with an Asymmetric Structure,” *Appl. Phys. Lett.*, vol. 71, 1997, pp. 1756-1758.
- [20] J. Seidel, S. Grafström, Ch. Loppacher, S. Trogisch, F. Schlaphof, and L.M. Eng, “Near-Field Spectroscopy with White-Light Illumination,” *Appl. Phys. Lett.*, vol. 79, 2001, pp. 2291-2293.



Kang-Ho Park received the BS, MS, PhD degrees in physics from Seoul National University, Seoul, Korea, in 1987, 1989, and 1994, respectively. Since 1994 he has been working at ETRI in Daejeon. His research interests are nano-technology and nano-data storage; currently his research work is the realization of nano-optical data storage using aperture probe techniques. He is a Director of Nano Optical Data Storage Center (NANO-DISC) financially supported by Ministry of Science and Technology under the R&D program for fusion strategy of advanced technology.



Jeongyong Kim received the BS degree in physics from Korea University in 1993, and the MS and PhD degrees in physics from University of Cincinnati in 1995 and 1998, respectively. He did his post-doc in University of Illinois at Urbana-Champaign before he joined ETRI in 2000. He has been with the Department of Physics in University of Incheon since 2002. His research interests are near-field optics and its applications including optical data storages using near-field probes.



Ki-Bong Song received the BS, MS and PhD degrees in physics from Sogang University in 1988, 1995 and 1999, respectively. He is currently working in ETRI. His research interests include nano-nonlinear optics, near-field optics and near-field recording in optical data storage.



Sung-Q Lee received the BS, MS, and PhD degrees in mechanical engineering from Korea Advanced Institute of Science and Technology (KAIST) in 1994, 1996 and 2001, respectively. In 2000, he worked as a Visiting Researcher at Michigan Technical University. Since 2001, he has worked in ETRI as a Research Staff. His main interests include precision actuator design and control, optical data storage device, SPM system implementation, and mechatronics.



Junho Kim received the BS, MS, and PhD degrees in physics from Korea Advanced Institute of Science and Technology in 1992, 1994 and 1998, respectively. From 1998 to 2000, he worked as a Post-Doctoral Researcher at Physics Department of University of California at San Diego. Since 2000, he has worked in ETRI as a Research Staff. His main interests include superconducting electronics, molecule-scale electronics, nano-fabrication, nano-scale characterization with SPM and NSOM.



Eun-Kyoung Kim received the MS, and PhD degrees from School of Physics, Seoul National University, Korea in 1995 and 2000, respectively. She joined ETRI in 2000. Her research interests include the MEMS devices for multifunctional NSOM probes, nanostorage devices, and nanoscale heat transports.